# Utility of Amino Acid PET in the Differential Diagnosis of Recurrent Brain Metastases and Treatment-Related Changes: A Meta-analysis

Timo Schlürmann[1], Birgit Waschulzik[2], Stephanie Combs[3–5], Jens Gempt[6], Benedikt Wiestler[7], Wolfgang Weber[1], and Igor Yakushev[1]

[1]*Department of Nuclear Medicine, School of Medicine, Klinikum Rechts der Isar, Technical University of Munich, Munich, Germany;* [2]*Institute of AI and Informatics in Medicine, School of Medicine, Klinikum Rechts der Isar, Technical University of Munich, Munich, Germany;* [3]*Department of Radiation Oncology, School of Medicine, Klinikum Rechts der Isar, Technical University of Munich, Munich, Germany;* [4]*Institute of Radiation Medicine at Helmholtz Zentrum München (HMGU), Oberschleißheim, Germany;* [5]*Deutsches Konsortium für Translationale Krebsforschung (DKTK), Partner Sites Munich, Freiburg, and Heidelberg;* [6]*Department of Neurosurgery, School of Medicine, Klinikum Rechts der Isar, Technical University of Munich, Munich, Germany; and* [7]*Department of Neuroradiology, School of Medicine, Klinikum Rechts der Isar, Technical University of Munich, Munich, Germany*

Amino acid PET is an established method to assist differential diagnosis of therapy-related changes versus recurrence in gliomas. However, its diagnostic value in brain metastases is yet to be determined. The goal of this study was to summarize evidence on the diagnostic utility of amino acid PET in recurrent brain metastases. **Methods:** The medical databases MEDLINE, EMBASE, and the Cochrane Library were screened for English-language studies with at least 10 patients who had undergone first-line treatment including radiotherapy and in whom a final diagnosis had been determined by histologic examination or imaging and clinical follow-up. Pooled estimates with 95% CIs were calculated. Heterogeneity was assessed using $I^2$ statistics. **Results:** Following the above criteria, 12 studies with the tracers methyl-[$^{11}$C]-methionine ($n = 6$), *O*-(2-[$^{18}$F]fluoroethyl)-L-tyrosine ($n = 3$), methyl-[$^{11}$C]-methionine and *O*-(2-[$^{18}$F]fluoroethyl)-L-tyrosine ($n = 1$), and 6-[$^{18}$F]fluoro-L-dopa ($n = 2$), with a total of 547 lesions in 397 patients, were included. Pooled sensitivity and specificity were 82% (95% CI, 76–86) and 84% (95% CI, 79–88), respectively. Pooled positive and negative predictive values were 84% (95% CI, 77–90) and 83% (95% CI, 77–88), respectively. Positive and negative likelihood ratios, and diagnostic odds ratio were 3.8 (95% CI 3.0–4.8), 0.3 (95% CI 0.2–0.3), and 16.7 (95% CI 10.8–25.9), respectively. Heterogeneity was overall low. **Conclusion:** The present meta-analysis indicates a good accuracy of amino acid PET in the differential diagnosis of recurrent brain metastases. In particular, specificity of 84% suggests that amino acid PET may reduce the number of invasive procedures and overtreatment in patients with treatment-related changes. This study provides class IIa evidence on the utility of amino acid PET in the differential diagnosis of recurrent brain metastases.

**Key Words:** PET; cerebral metastases; radiation therapy; radiation necrosis; pseudoprogression

**J Nucl Med 2023; 64:816–821**
DOI: 10.2967/jnumed.122.264803

Brain metastases occur in 20%–40% of all tumor patients (*1*). The primary tumors most likely to metastasize to the brain are bronchial carcinoma (40%–50%), breast carcinoma (15%–20%), malignant melanoma (5%–20%), renal cancer (5%–10%), and cancers of the gastrointestinal tract (5%) (*2*). Management of patients with brain metastases usually includes surgery, radiation, and chemotherapy. Therapy is selected on an individual basis, taking into account the primary tumor and location, and number of metastases. Still, most patients with cerebral metastases receive primary, concomitant, or curative radiotherapy during the disease course. After radiation treatment, patients are followed clinically and radiographically with serial MRI. Some develop treatment-related changes (TRCs) such as radiation necrosis and pseudoprogression (*3*). The true incidence of TRCs is hard to estimate, with values varying widely in the literature, depending on diagnostic criteria, duration of follow-up, radiation modality, and regimen. Radiation necrosis may underlie up to half of lesions that progress radiologically after stereotactic radiosurgery (*4,5*). Differentiation between recurrent or progressive brain metastasis (RPBM) and TRCs is challenging. Both can manifest with similar clinical symptoms and MRI features, such as rimlike contrast enhancement, perilesional edema, and central hypointensity on T2-weighted imaging (*6*). For this clinical question, conventional MRI was shown to deliver a pooled sensitivity and specificity of 76% and 59%, respectively (*7*). As the management of patients with RPBM versus TRCs differs (*4*), accurate and early differential diagnosis is essential.

Originally, $^{18}$F-FDG was used to differentiate benign and low-grade tumors from high-grade tumors (*8*). However, the utility of $^{18}$F-FDG PET was shown to be limited by high uptake in normal gray matter and nonspecific uptake in inflammatory lesions (*9*). Amino acid PET takes advantage of the fact that brain malignancies often overexpress amino acid transport proteins. Common amino acid tracers include methyl-[$^{11}$C]-methionine ($^{11}$C-MET), 6-[$^{18}$F]fluoro-L-dopa ($^{18}$F-FDOPA), and *O*-(2-[$^{18}$F]fluoroethyl)-L-tyrosine ($^{18}$F-FET).

In recent years, several single-center studies have investigated the utility of amino acid PET in the differential diagnosis of recurrent brain metastases. The aim of the present work was to summarize existing evidence in the form of a meta-analysis.

Received Dec. 27, 2021; revision accepted Nov. 28, 2022.
For correspondence or reprints, contact Igor Yakushev (igor.yakushev@tum.de).
Published online Dec. 2, 2022.

## MATERIALS AND METHODS

A literature search was performed in the online medical databases MEDLINE (via PubMed), EMBASE, the Cochrane Library (Cochrane Central Register of Controlled Trials), and Google Scholar. The search was limited to studies on humans. The following key words were used: *Positron Emission Tomography; PET* AND *recurrence, recurrent, relapse, neoplasm, metastasis, metastatic progression* AND *radionecrosis, radiation necrosis, radiation-induced necrosis, posttreatment necrosis, radiation injury, radionecrotic, postradiotherapy necrosis* AND *radiation therapy, radiation treatment, radiosurgery*. The searches were performed in various combinations, both with "AND" and "OR." The last search was performed on December 1, 2021.

### Inclusion Criteria

Studies in English with at least 10 patients who had received PET with amino acid tracers for differentiation of RPBM from TRCs after radiotherapy were included. In addition, follow-up data had to allow creation of a contingency table. Histologic examination or continuous follow-up with radiologic imaging and clinical findings served as reference standards for the final diagnosis. Due to lack of information about primary tumors and clinical outcomes at a single-subject level in most studies, a differential analysis according to the primary tumor was impossible. Figure 1 depicts a flowchart of the selection procedure.

### Data Extraction

The following data were extracted from the included studies: first author, publication year, tracers, number of patients, number of lesions, number of true-positives, number of true-negatives, number of false-positives, and number of false-negatives. The calculation of the endpoints was based on the number of lesions. Some studies in addition provided estimates from kinetic analyses (*10,11*), but for consistency, only estimates of tumor-to-background ratio (TBR) were considered. If studies provided both mean TBR and maximum TBR, we considered mean TBR only, as the threshold was based on mean TBR in most overviewed studies (Table 2 of Galldiks et al. (*12*)). To assess the quality of the selected studies, we used Quality Assessment of Diagnostic Accuracy Studies 2 (*13*).

### Statistics

Common and random-effects bivariate models were used. Heterogeneity was assessed using $I^2$ statistics (the percentage of variation across studies that is due to heterogeneity rather than chance). Pooled estimates of sensitivity, specificity, and predictive values, as well as positive likelihood ratio (posLR), negative likelihood ratio (negLR), and diagnostic odds ratio (DOR) with 95% CIs, were calculated. PosLR above 3.0 were considered acceptable, above 10.0 good; NegLR below 0.3 were considered acceptable, below 0.1 good (*14*). DOR is used as an indicator of the effectiveness of medical tests with a binary classification. Values for DOR may range from zero to infinity; higher values indicate better test performance. DOR values above 1.0 are considered good (*14*). All statistical analyses were performed using the statistical software R, version 4.0.4 (*15*), with the meta (*16*) and mada (*17*) packages.

## RESULTS

Twelve studies were included in the meta-analysis (Table 1). These were performed with the tracers $^{11}$C-MET ($n$ = 6), $^{18}$F-FET ($n$ = 3), both $^{18}$F-FET and $^{11}$C-MET ($n$ = 1), and $^{18}$F-FDOPA ($n$ = 2). Although other amino acid tracers have been used in neurooncology, for example, α-[$^{11}$C]-methyl-L-tryptophan, they have not been applied with the above clinical question (*18*). Of 18 selected full-text articles (Fig. 1), six had to be excluded: one study with the tracer $^{18}$F-fluciclovine (*19*) was too small, that is, fewer than 10 patients; one study was limited to pseudoprogression (*20*); and one dealt with a cost-effectiveness analysis (*21*). Two further studies (*22,23*) had to be excluded because of overlapping patient cohorts. One more study was excluded (*24*), because reported data did not allow creation of a contingency table.

Finally, twelve studies (*10,11,25–34*) with a total of 397 patients with 547 lesions were assessed (Table 1). Overall, 269 lesions (49%) were found to be RPBM.

Supplemental Table 1 summarizes the methodologic quality of the selected studies (supplemental materials are available at http://jnm.snmjournals.org). Overall, the study quality can be regarded as moderate. In each of the 12 included studies, the time point of tracer injection and the time period of data acquisition meet the recent practice guidelines of the European Association of Nuclear Medicine, the European Association of Neurooncology, and the working group for Response Assessment in Neurooncology

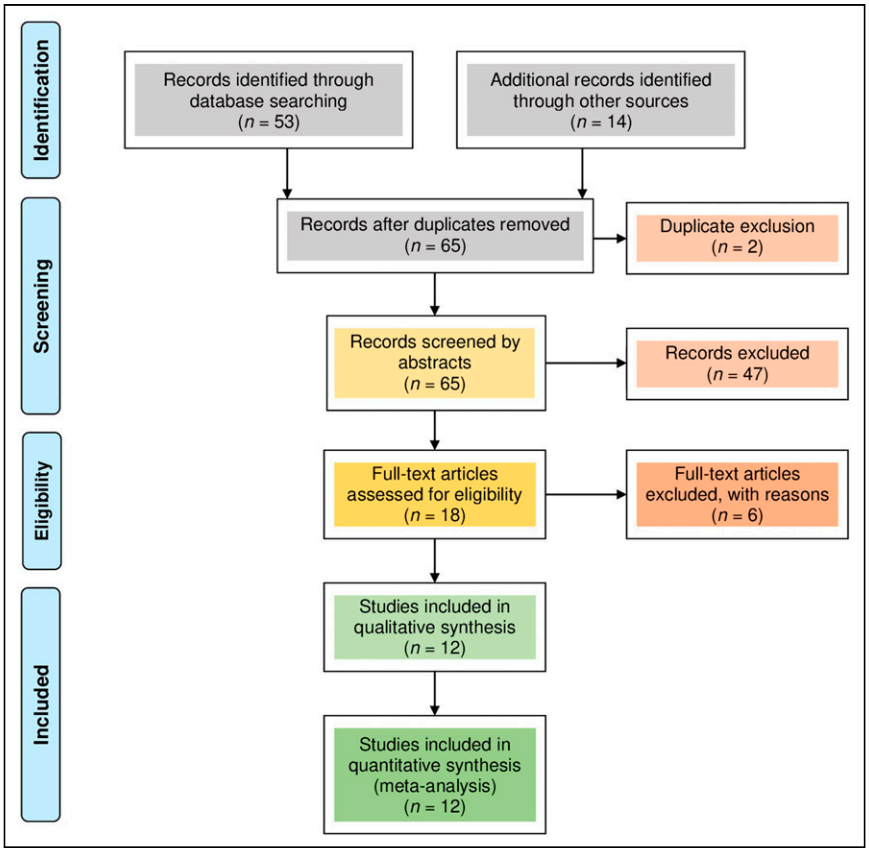


**FIGURE 1.** Identification of studies as PRISMA (Preferred Reporting Items for Systematic Reviews and Meta-Analyses) flow diagram.

**TABLE 1**
Study Characteristics

| Study | Tracer | Patients (*n*) | Lesions (*n*) | Sens (%) | Spec (%) | TP (*n*) | TN (*n*) | FP (*n*) | FN (*n*) | Acc (%) | PPV (%) | NPV (%) |
|---|---|---|---|---|---|---|---|---|---|---|---|---|
| Tsuyuguchi et al., 2003 | $^{11}$C-MET | 21 | 21 | 78 | 100 | 7 | 12 | 0 | 2 | 91 | 100 | 86 |
| Terakawa et al., 2008 | $^{11}$C-MET | 51 | 56 | 79 | 75 | 19 | 24 | 8 | 5 | 77 | 70 | 83 |
| Minamimoto et al., 2015 | $^{11}$C-MET | 39 | 42 | 82 | 86 | 23 | 12 | 2 | 5 | 83 | 92 | 71 |
| Jung et al., 2017 | $^{11}$C-MET | 48 | 77 | 71 | 81 | 36 | 21 | 5 | 15 | 74 | 88 | 58 |
| Tomura et al., 2017 | $^{11}$C-MET | 15 | 18 | 90 | 75 | 9 | 6 | 2 | 1 | 83 | 82 | 86 |
| Yomo et al., 2017 | $^{11}$C-MET | 32 | 37 | 82 | 75 | 14 | 15 | 5 | 3 | 78 | 74 | 83 |
| Grosu et al., 2011 | $^{11}$C-MET, $^{18}$F-FET | 13 | 10 | 83 | 100 | 5 | 4 | 0 | 1 | 90 | 100 | 80 |
| Romagna et al., 2016 | $^{18}$F-FET | 21 | 50 | 86 | 79 | 18 | 23 | 6 | 3 | 82 | 75 | 88 |
| Ceccon et al., 2017 | $^{18}$F-FET | 62 | 76 | 86 | 88 | 31 | 35 | 5 | 5 | 87 | 86 | 88 |
| Galldiks et al., 2021 | $^{18}$F-FET | 21 | 31 | 73 | 94 | 11 | 15 | 1 | 4 | 84 | 92 | 79 |
| Lizarraga et al., 2014 | $^{18}$F-FDOPA | 32 | 83 | 81 | 73 | 26 | 37 | 14 | 6 | 76 | 65 | 86 |
| Cicone et al., 2015 | $^{18}$F-FDOPA | 42 | 46 | 90 | 92 | 18 | 24 | 2 | 2 | 91 | 90 | 92 |

Sens = sensitivity; Spec = specificity; TP = true-positives; TN = true-negatives; FP = false-positives; FN = false-negatives; Acc = accuracy; PPV = positive predictive value; NPV = negative predictive value

with PET (*35*). The cutoffs and verification method (histologic confirmation vs. clinical–neuroradiologic follow-up) of the selected studies are summarized in Table 2.

As shown in Figure 2, the heterogeneity among the studies regarding sensitivity appeared to be an $I^2$ of 0%. Consequently, the common-effect and random-effect models provided identical results for pooled sensitivity of 0.82 (95% CI, 0.76–0.86).

The analyses of specificity are summarized in Figure 3. An $I^2$ of 25% means that 25% of the variability is explained by heterogeneity among the studies. This resulted in an identical estimate for pooled specificity but a slightly different estimate for 95% CI in the common-effect and random-effect models: 0.84 (95% CI, 0.79–0.88) and 0.84 (95% CI, 0.78–0.90), respectively. Table 3 summarizes the values of DOR and likelihood ratios. DOR was 16.7 (95% CI, 10.8–25.9)—that is, good. PosLR and negLR were 3.8 (95% CI, 3.0–4.8) and 0.3 (95% CI, 0.2–0.3), respectively—that is, both within the acceptable range (*14*).

**TABLE 2**
Cutoffs and Verification Method (Histologic Confirmation vs. Clinical–Neuroradiologic Follow-up) as Percentage of Histologic Confirmation

| Study | Tracer | Mean TBR cutoff | Maximum TBR cutoff | Histologic confirmation, % (lesions)* |
|---|---|---|---|---|
| Tsuyuguchi et al., 2003 | $^{11}$C-MET | 1.40 | | 52 |
| Terakawa et al., 2008 | $^{11}$C-MET | 1.40 | | 54 |
| Minamimoto et al., 2015 | $^{11}$C-MET | | 1.30 | Not reported |
| Jung et al., 2017 | $^{11}$C-MET | | 1.61 | 12 |
| Tomura et al., 2017 | $^{11}$C-MET | | 1.42 | 56 |
| Yomo et al., 2017 | $^{11}$C-MET | | 1.40 | 41 |
| Grosu et al., 2011 | $^{11}$C-MET | | 1.80 | 50 |
| Grosu et al., 2011 | $^{18}$F-FET | | 1.80 | 50 |
| Romagna et al., 2016 | $^{18}$F-FET | 1.95 | 2.15 | 40 |
| Ceccon et al., 2017 | $^{18}$F-FET | 1.95 | 2.55 | 34 |
| Galldiks et al., 2021 | $^{18}$F-FET | 1.95 | | 3 |
| Lizarraga et al., 2014 | $^{18}$F-FDOPA | 1.70 | 2.02 | 11 |
| Cicone et al., 2015 | $^{18}$F-FDOPA | | 1.59 | 24 |

*Percentages, at the level of lesions (not patients).

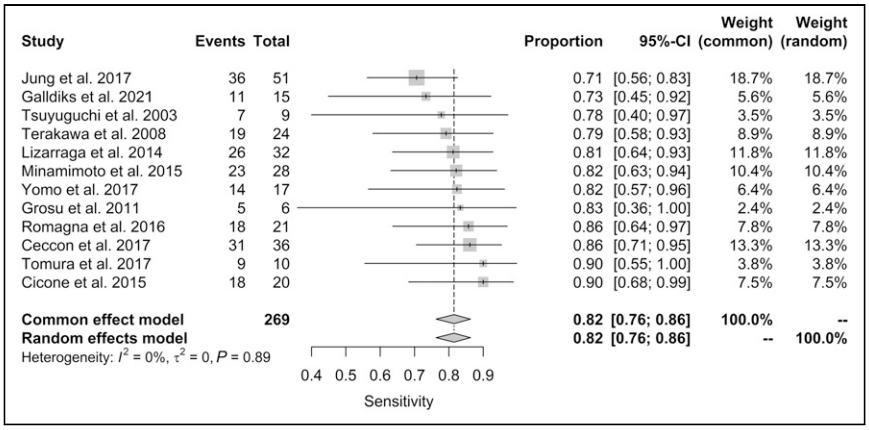


**FIGURE 2.** Forest plot for sensitivity. Events column lists the number of true-positives. Total column shows sum of true-positives and false-negatives. Proportion column lists reported sensitivity of individual publications and 95% CI. Weight columns indicate contribution of given study according to sample size. Area of gray squares is proportional to weight of study in the meta-analysis. Length of diamonds corresponds to corresponding CI. Vertical line represents pooled sensitivity.

Pooled diagnostic accuracy was 0.82 (95% CI, 0.78–0.85). Pooled positive and negative predictive values were 84% (95% CI, 77–90) and 83% (95% CI, 77–88), respectively. A summary receiver-operating characteristic curve as calculated using the bivariate model is shown in Supplemental Figure 1. Because the biodistribution of $^{18}$F-FDOPA differs from that of $^{11}$C-MET and $^{18}$F-FET, we in addition performed the same analyses only for studies with $^{11}$C-MET and $^{18}$F-FET ($n$ = 10). The results did not change substantially (Supplemental Figs. 2 and 3; Supplemental Table 2). There was also no statistically significant difference between the studies with $^{11}$C-MET and $^{18}$F-FET (data not shown).

## DISCUSSION

To our knowledge, this is the first meta-analysis on the utility of amino acid PET in the differential diagnosis of RPBM and TRCs. It includes 12 studies with a total of 547 lesions in 397 patients. Using histologic examination or radiologic and clinical follow-up as reference, we found a pooled sensitivity and specificity of 82% and 84%, respectively. Although values for posLR and negLR were acceptable, DOR appeared to be good.

As compared with gliomas, sensitivity of amino acid PET for differentiation of RPBM from TRCs seems to be lower. In particular, a recent meta-analysis of 39 studies with amino acid PET (*36*) reported a sensitivity of 85%–93% and specificity of 82%–100%, depending on the tracer, that is, $^{18}$F-FET, $^{11}$C-MET, or $^{18}$F-FDOPA. Given a large variance in the amino acid transporter expression of brain metastases (*37*), some might primarily be PET-negative. Yet, despite a large variance in $^{18}$F-FET uptake, most (89%) newly diagnosed and untreated brain metastases were reported to be PET-positive (*38*). Another explanation of the lower sensitivity is the impact of systemic therapy; that is, some agents may reduce tumor vitality or amino acid transporter expression. In this regard, it is noticeable that one of the lowest sensitivities (73%) among the included studies was in patients who had undergone immune checkpoint inhibition and targeted therapy (*11*). The impact of this modern, increasingly available therapy on tracer uptake warrants further studies. We found a pooled diagnostic specificity of 84%, which is well within the range of values reported for gliomas (*36*). That is, TRCs are more likely to be PET-negative. Similar to gliomas, however, specificity is far from perfect, as inflammatory processes such as reactive astrocytosis after radiation therapy or immunotherapy may result in tracer uptake above the level of normal brain tissue (*39*), in some cases leading to false-positive findings on PET (*40*). Pooled positive and negative predictive values were 84% and 83%, respectively. Although, from a clinical perspective, positive and negative predictive values are more helpful for decision making than conventional sensitivity and specificity, the former indices are dependent on the prevalence of a pathologic condition—that is, recurrent brain metastases in the included studies. Therefore, these results should be treated with caution.

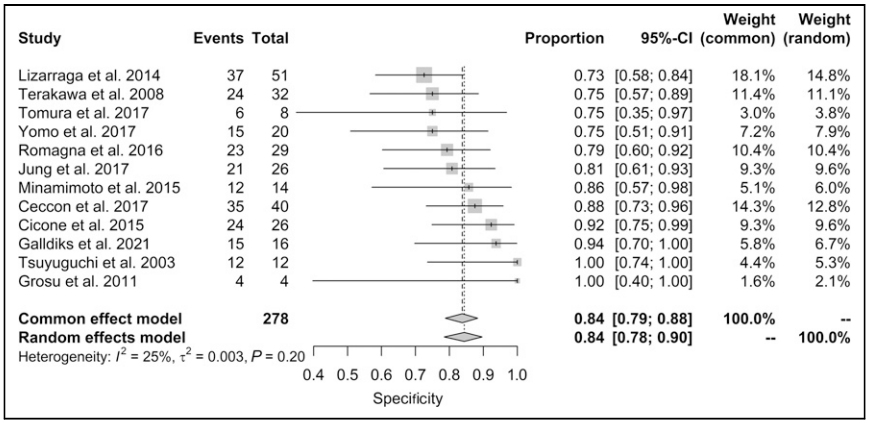


**FIGURE 3.** Forest plot for specificity. Events column lists the number of true-negatives. Total column shows sum of true-negatives and false-positives. Proportion column lists reported specificity of individual publications and 95% CI. Weight columns indicate contribution of given study according to sample size. Area of gray squares is proportional to weight of study in the meta-analysis. Length of diamonds corresponds to corresponding CI. Vertical line represents pooled specificity.

So far, just one meta-analysis has addressed the diagnostic utility of PET in the differentiation between RPBM and TRCs (*41*). Yet, that work analyzed a pool of studies ($n$ = 15) with $^{18}$F-FDG ($n$ = 6) and amino acid tracers ($n$ = 9) without a separate analysis for the latter. Among these 9 studies, only 5 fulfilled our selection criteria and were therefore included in the present work (*10,31–34*). Thus, the current meta-analysis includes substantially more studies and coveres the amino acid tracers only, following recent recommendations of the RANO/PET group on PET imaging in patients with brain metastasis (*12*). Because of a low lesion-to-background ratio, that report rated $^{18}$F-FDG PET as a test with limited diagnostic accuracy (Table 3 of Galldiks et al. (*12*)).

This study had certain limitations. Because brain metastases are often multifocal, and biopsy or resection is usually performed on

**TABLE 3**
Pooled Estimates of DOR, Positive Likelihood Ratio (posLR), and Negative Likelihood Ratio (negLR) with Corresponding 95% CIs

| | | DOR | | | posLR | | | negLR | | |
|---|---|---|---|---|---|---|---|---|---|---|
| | | | 95% CI | | | 95% CI | | | 95% CI | |
| Study | Tracer | Value | 2.5% | 97.5% | Value | 2.5% | 97.5% | Value | 2.5% | 97.5% |
| Tsuyuguchi et al., 2003 | $^{11}$C-MET | 75.00 | 3.16 | 1782.78 | 19.50 | 1.26 | 302.43 | 0.26 | 0.09 | 0.77 |
| Terakawa et al., 2008 | $^{11}$C-MET | 10.22 | 3.00 | 34.84 | 3.03 | 1.64 | 5.60 | 0.3 | 0.14 | 0.64 |
| Minamimoto et al., 2015 | $^{11}$C-MET | 21.36 | 4.12 | 110.68 | 4.86 | 1.55 | 15.28 | 0.23 | 0.10 | 0.50 |
| Jung et al., 2017 | $^{11}$C-MET | 9.21 | 3.04 | 27.91 | 3.45 | 1.60 | 7.42 | 0.37 | 0.24 | 0.59 |
| Tomura et al., 2017 | $^{11}$C-MET | 16.47 | 1.72 | 157.29 | 3.11 | 1.06 | 9.15 | 0.19 | 0.04 | 0.88 |
| Yomo et al., 2017 | $^{11}$C-MET | 11.68 | 2.55 | 53.35 | 3.08 | 1.45 | 6.53 | 0.26 | 0.10 | 0.70 |
| Grosu et al., 2011 | $^{18}$F-FET/$^{11}$C-MET | 33.00 | 1.06 | 1023.56 | 7.86 | 0.55 | 112.09 | 0.24 | 0.06 | 1.01 |
| Romagna et al., 2016 | $^{18}$F-FET | 19.11 | 4.55 | 80.27 | 3.88 | 1.92 | 7.85 | 0.20 | 0.08 | 0.54 |
| Ceccon et al., 2017 | $^{18}$F-FET | 36.97 | 10.32 | 132.37 | 6.35 | 2.88 | 13.97 | 0.17 | 0.08 | 0.37 |
| Galldiks et al., 2021 | $^{18}$F-FET | 26.41 | 3.58 | 194.96 | 8.15 | 1.71 | 38.71 | 0.31 | 0.14 | 0.69 |
| Lizarraga et al., 2014 | $^{18}$F-FDOPA | 10.54 | 3.69 | 30.14 | 2.88 | 1.80 | 4.60 | 0.27 | 0.13 | 0.56 |
| Cicone et al., 2015 | $^{18}$F-FDOPA | 72.52 | 11.36 | 463.10 | 9.51 | 2.89 | 31.31 | 0.13 | 0.04 | 0.42 |
| Summary* | All | 16.73 | 10.79 | 25.93 | 3.75 | 2.95 | 4.77 | 0.27 | 0.21 | 0.34 |

*Random-effects estimates.

single lesions, radiologic and clinical criteria were used as a reference for more than two thirds of lesions. Second, the included studies varied widely regarding the follow-up duration (range, 3–23 mo). Third, most studies did not report the lesion size. Thus, it remains unclear how far the reported values of sensitivity might have been compromised by partial-volume effects in small lesions. In this respect, the maximal diameter of contrast enhancement in T1-weighted MRI (10 mm)—that is, at least double the spatial resolution (full width at half maximum) of modern PET scanners—was proposed as the minimal lesion size (*29*). Fourth, although we carefully checked for patient overlap, it cannot be excluded (*26,28*). Finally, most studies had a retrospective design.

## CONCLUSION

The present meta-analysis suggestes good accuracy for amino acid PET in the differential diagnosis of recurrent brain metastases. In particular, specificity of 84% indicates that amino acid PET may reduce the number of invasive procedures and overtreatment in patients with TRCs. This study provides class IIa evidence on the utility of amino acid PET in the differential diagnosis of RPBM. Further studies—preferably multicenter ones—should investigate the dependence of tracer uptake on the origin, histologic type, and molecular biomarkers of the primary tumor, as well as on the character and regime of local and systemic therapy.

## DISCLOSURE

Igor Yakushev has received consultant or lecture fees from ABX-CRO, Blue Earth Diagnostics, and Piramal, as well as grants from the Alzheimer Research Initiative Germany, the German Research Foundation (DFG), and the Federal Ministry of Education and Research Germany (BMBF). No other potential conflict of interest relevant to this article was reported.

**KEY POINTS**

**QUESTION:** How accurate is amino acid PET in the differential diagnosis of recurrent brain metastases and TRCs?

**PERTINENT FINDINGS:** The present study summarized, in the form of a meta-analysis, the existing evidence on the diagnostic utility of amino acid PET in recurrent brain metastases. Across 12 included studies, pooled sensitivity and specificity were 82% and 84%, respectively.

**IMPLICATIONS FOR PATIENT CARE:** Amino acid PET is able to assist the differential diagnosis of recurrent brain metastases versus TRCs.

## REFERENCES

1. Gavrilovic IT, Posner JB. Brain metastases: epidemiology and pathophysiology. *J Neurooncol.* 2005;75:5–14.
2. Ostrom QT, Wright CH, Barnholtz-Sloan JS. Brain metastases: epidemiology. *Handb Clin Neurol.* 2018;149:27–42.
3. Dietrich J, Winter SF, Klein JP. Neuroimaging of brain tumors: pseudoprogression, pseudoresponse, and delayed effects of chemotherapy and radiation. *Semin Neurol.* 2017;37:589–596.
4. Narloch JL, Farber SH, Sammons S, et al. Biopsy of enlarging lesions after stereotactic radiosurgery for brain metastases frequently reveals radiation necrosis. *Neuro Oncol.* 2017;19:1391–1397.
5. Fujimoto D, von Eyben R, Gibbs IC, et al. Imaging changes over 18 months following stereotactic radiosurgery for brain metastases: both late radiation necrosis and tumor progression can occur. *J Neurooncol.* 2018;136:207–212.

6. Thust SC, van den Bent MJ, Smits M. Pseudoprogression of brain tumors. *J Magn Reson Imaging.* 2018;48:571–589.
7. Suh CH, Kim HS, Jung SC, Choi CG, Kim SJ. Comparison of MRI and PET as potential surrogate endpoints for treatment response after stereotactic radiosurgery in patients with brain metastasis. *AJR.* 2018;211:1332–1341.
8. Delbeke D, Meyerowitz C, Lapidus RL, et al. Optimal cutoff levels of F-18 fluorodeoxyglucose uptake in the differentiation of low-grade from high-grade brain tumors with PET. *Radiology.* 1995;195:47–52.
9. Salber D, Stoffels G, Pauleit D, et al. Differential uptake of *O*-(2-$^{18}$F-fluoroethyl)-L-tyrosine, L-$^{3}$H-methionine, and $^{3}$H-deoxyglucose in brain abscesses. *J Nucl Med.* 2007;48:2056–2062.
10. Ceccon G, Lohmann P, Stoffels G, et al. Dynamic O-(2-$^{18}$F-fluoroethyl)-L-tyrosine positron emission tomography differentiates brain metastasis recurrence from radiation injury after radiotherapy. *Neuro Oncol.* 2017;19:281–288.
11. Galldiks N, Abdulla DSY, Scheffler M, et al. Treatment monitoring of immunotherapy and targeted therapy using $^{18}$F-FET PET in patients with melanoma and lung cancer brain metastases: initial experiences. *J Nucl Med.* 2021;62:464–470.
12. Galldiks N, Langen K-J, Albert NL, et al. PET imaging in patients with brain metastasis: report of the RANO/PET group. *Neuro Oncol.* 2019;21:585–595.
13. Whiting PF, Rutjes AWS, Westwood ME, et al. QUADAS-2: a revised tool for the quality assessment of diagnostic accuracy studies. *Ann Intern Med.* 2011;155:529–536.
14. Higgins JPT, Thompson SG, Deeks JJ, Altman DG. Measuring inconsistency in meta-analyses. *BMJ.* 2003;327:557–560.
15. R Core Team (2020). European Environment Agency website. https://www.eea.europa.eu/data-and-maps/indicators/oxygen-consuming-substances-in-rivers/r-development-core-team-2006. Accessed January 19, 2023.
16. Balduzzi S, Rücker G, Schwarzer G. How to perform a meta-analysis with R: a practical tutorial. *Evid Based Ment Health.* 2019;22:153–160.
17. Doebler P, Holling H. Sousa-Pinto B. Meta-analysis of diagnostic accuracy with mada. The Comprehensive R Archive Network website. https://cran.r-project.org/web/packages/mada/vignettes/mada.pdf. Accessed January 19, 2023.
18. Bosnyák E, Kamson DO, Robinette NL, Barger GR, Mittal S, Juhász C. Tryptophan PET predicts spatial and temporal patterns of post-treatment glioblastoma progression detected by contrast-enhanced MRI. *J Neurooncol.* 2016;126:317–325.
19. Parent EE, Patel D, Nye JA, et al. [$^{18}$F]-fluciclovine PET discrimination of recurrent intracranial metastatic disease from radiation necrosis. *EJNMMI Res.* 2020;10:148.
20. Akhoundova D, Hiltbrunner S, Mader C, et al. $^{18}$F-FET PET for diagnosis of pseudoprogression of brain metastases in patients with non-small cell lung cancer. *Clin Nucl Med.* 2020;45:113–117.
21. Heinzel A, Müller D, Yekta-Michael SS, et al. *O*-(2-$^{18}$F-fluoroethyl)-L-tyrosine PET for evaluation of brain metastasis recurrence after radiotherapy: an effectiveness and cost-effectiveness analysis. *Neuro Oncol.* 2017;19:1271–1278.
22. Galldiks N, Stoffels G, Filss CP, et al. Role of *O*-(2-$^{18}$F-fluoroethyl)-L-tyrosine PET for differentiation of local recurrent brain metastasis from radiation necrosis. *J Nucl Med.* 2012;53:1367–1374.
23. Lohmann P, Stoffels G, Ceccon G, et al. Radiation injury vs. recurrent brain metastasis: combining textural feature radiomics analysis and standard parameters may increase $^{18}$F-FET PET accuracy without dynamic scans. *Eur Radiol.* 2017;27:2916–2927.
24. Okamoto S, Shiga T, Hattori N, et al. Semiquantitative analysis of C-11 methionine PET may distinguish brain tumor recurrence from radiation necrosis even in small lesions. *Ann Nucl Med.* 2011;25:213–220.
25. Tomura N, Kokubun M, Saginoya T, Mizuno Y, Kikuchi Y. Differentiation between treatment-induced necrosis and recurrent tumors in patients with metastatic brain tumors: comparison among $^{11}$C-methionine-PET, FDG-PET, MR permeability imaging, and MRI-ADC-preliminary results. *AJNR.* 2017;38:1520–1527.
26. Jung T-Y, Kim I-Y, Lim S-H, et al. Optimization of diagnostic performance for differentiation of recurrence from radiation necrosis in patients with metastatic brain tumors using tumor volume-corrected $^{11}$C-methionine uptake. *EJNMMI Res.* 2017;7:45.
27. Minamimoto R, Saginoya T, Kondo C, et al. Differentiation of brain tumor recurrence from post-radiotherapy necrosis with $^{11}$C-methionine PET: visual assessment versus quantitative assessment. *PLoS One.* 2015;10:e0132515.
28. Yomo S, Oguchi K. Prospective study of $^{11}$C-methionine PET for distinguishing between recurrent brain metastases and radiation necrosis: limitations of diagnostic accuracy and long-term results of salvage treatment. *BMC Cancer.* 2017;17:713.
29. Grosu A-L, Astner ST, Riedel E, et al. An interindividual comparison of O-(2-[$^{18}$F]fluoroethyl)-L-tyrosine (FET)- and L-[methyl-$^{11}$C]methionine (MET)-PET in patients with brain gliomas and metastases. *Int J Radiat Oncol Biol Phys.* 2011;81:1049–1058.
30. Tsuyuguchi N, Sunada I, Iwai Y, et al. Methionine positron emission tomography of recurrent metastatic brain tumor and radiation necrosis after stereotactic radiosurgery: is a differential diagnosis possible? *J Neurosurg.* 2003;98:1056–1064.
31. Romagna A, Unterrainer M, Schmid-Tannwald C, et al. Suspected recurrence of brain metastases after focused high dose radiotherapy: can [$^{18}$F]FET-PET overcome diagnostic uncertainties? *Radiat Oncol.* 2016;11:139.
32. Lizarraga KJ, Allen-Auerbach M, Czernin J, et al. $^{18}$F-FDOPA PET for differentiating recurrent or progressive brain metastatic tumors from late or delayed radiation injury after radiation treatment. *J Nucl Med.* 2014;55:30–36.
33. Cicone F, Minniti G, Romano A, et al. Accuracy of F-DOPA PET and perfusion-MRI for differentiating radionecrotic from progressive brain metastases after radiosurgery. *Eur J Nucl Med Mol Imaging.* 2015;42:103–111.
34. Terakawa Y, Tsuyuguchi N, Iwai Y, et al. Diagnostic accuracy of $^{11}$C-methionine PET for differentiation of recurrent brain tumors from radiation necrosis after radiotherapy. *J Nucl Med.* 2008;49:694–699.
35. Law I, Albert NL, Arbizu J, et al. Joint EANM/EANO/RANO practice guidelines/SNMMI procedure standards for imaging of gliomas using PET with radiolabelled amino acids and [$^{18}$F]FDG: version 1.0. *Eur J Nucl Med Mol Imaging.* 2019;46:540–557.
36. de Zwart PL, van Dijken BRJ, Holtman GA, et al. Diagnostic accuracy of PET tracers for the differentiation of tumor progression from treatment-related changes in high-grade glioma: a systematic review and metaanalysis. *J Nucl Med.* 2020;61:498–504.
37. Papin-Michault C, Bonnetaud C, Dufour M, et al. Study of LAT1 expression in brain metastases: towards a better understanding of the results of positron emission tomography using amino acid tracers. *PLoS One.* 2016;11:e0157139.
38. Unterrainer M, Galldiks N, Suchorska B, et al. $^{18}$F-FET PET uptake characteristics in patients with newly diagnosed and untreated brain metastasis. *J Nucl Med.* 2017;58:584–589.
39. Piroth MD, Prasath J, Willuweit A, et al. Uptake of O-(2-[$^{18}$F]fluoroethyl)-L-tyrosine in reactive astrocytosis in the vicinity of cerebral gliomas. *Nucl Med Biol.* 2013;40:795–800.
40. Langen KJ, Stoffels G, Filss C, et al. Imaging of amino acid transport in brain tumours: positron emission tomography with O-(2-[$^{18}$F]fluoroethyl)-L-tyrosine (FET). *Methods.* 2017;130:124–134.
41. Li H, Deng L, Bai HX, et al. Diagnostic accuracy of amino acid and FDG-PET in differentiating brain metastasis recurrence from radionecrosis after radiotherapy: a systematic review and meta-analysis. *AJNR.* 2018;39:280–288.